Numerical-differentiation approach for the ground state of the He atom*

Rashad M. Shoucri and Byron T. Darling
Département de Physique, Université Laval, Québec, G1K 7P4, Canada
(Received 4 June 1975)

The method of numerical differentiation is applied to solve the coupled set of ordinary differential equations for a three-body system derived in the previous paper. This is done for the ground state of the He atom. The matching of the forward and backward numerical solutions of the coupled system of differential equations is achieved by repeated applications of Newton's correction method. The matching of up to 16 coupled curves is carried out successfully, but the results obtained show that a very large number of coupled terms are required to obtain a good convergence of the ground-state energy.

INTRODUCTION

In the previous paper[1] (to be referred to as I), a coupled set of ordinary differential equations for the calculation of the energy of a three-body system was derived. This coupled self-adjoint set is given by

$$\left(\frac{d^2}{dR^2}+2E+\frac{C^{\nu\nu}_{\kappa\kappa}}{R}-\frac{(\kappa+\frac{3}{2})(\kappa+\frac{5}{2})}{R^2}\right)\chi^{\nu}_{\kappa}(R) = -\frac{1}{R}\sum_{\kappa',\nu'} C^{\nu\nu'}_{\kappa\kappa'}\chi^{\nu'}_{\kappa'}(R)\,, \quad (1)$$

where $C^{\nu\nu'}_{\kappa\kappa'}/R$ are the matrix elements for the Coulomb interaction derived in Appendix A. In this paper, we apply Eqs. (1) to the calculation of the atomic ground-state energy of He by using the method of numerical differentiation. The purpose of the study is (i) to study the number of coupled equations required to make the energy converge. Few numerical results are available to give a full appreciation of the method of hyperspherical harmonics (h.h.). Simonov[2] has done a study of the problem of the triton, and Brayshaw and Buck[3] have done similar calculations of the nuclear binding energy of ^{3}H and ^{3}He. Both works state that only four h.h. or less are sufficient to give a good approximation of the wave function, and Ref. 3 indicates a surprisingly good agreement between theory and experiment. Erens *et al.*,[4] on the contrary, and Bruinsma and Van Wageningen,[5] have made some extensive calculations on the triton, and they report that the low-order h.h. might seem to approximate the wave function, while indeed a very large number of these h.h. is required to give a good convergence of the energy value. All these previous studies use the variational principle, which is not the method used in this article.

(ii) The second purpose of the present study is to investigate the possiblity of using the method of numerical differentiation to calculate the ground-state energy of He. A previous attempt was made by Winter *et al.*,[6] who derived a coupled set of partial differential equations in the two variables r_1 and r_2 (r_1 and r_2 are the respective distances of the two electrons to the nucleus). Because of this two dimensionality, the number of pivotal points needed to achieve the required accuracy was prohibitive, and the energy value was calculated by using numerical extrapolation. The coupled set of ordinary differential equations (1) suggests the possiblity of trying once more the method of numerical differentiation. The low cycle time and high storage capacity of modern computers make such an effort tempting. This method not only computes the energy but also produces the numerical values of the radial coupled solutions, provided only that proper boundary conditions are assumed. This avoids the approximative trial methods used until now in the literature to try to determine some analytic expression for the wave function of the He problem.

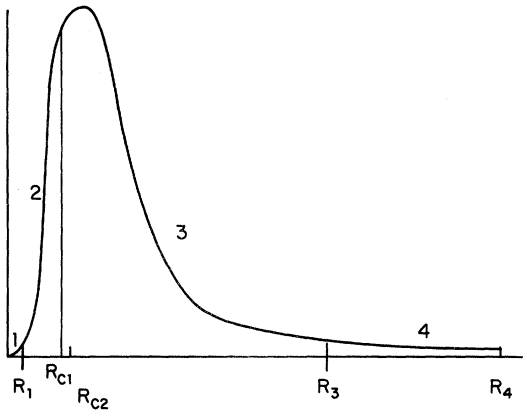

FIG. 1. Different regions along a radial curve correspond to different mesh sizes used to carry out the numerical differentiation process.

NUMERICAL PROCEDURE

The transformation of a coupled set of differential equations into a coupled set of difference equations has been discussed by several authors.[7,8] The method of Noumerov[7] is used, and one obtains

$$\left[1+\tfrac{1}{12}h^2\left(\frac{C^{\nu\nu}_{\kappa\kappa}}{R-h}-\frac{(\kappa+\frac{3}{2})(\kappa+\frac{5}{2})}{(R-h)^2}\right)\right]\chi^{\nu}_{\kappa}(R-h)+\left[-2+\tfrac{5}{6}h^2\left(\frac{C^{\nu\nu}_{\kappa\kappa}}{R}-\frac{(\kappa+\frac{3}{2})(\kappa+\frac{5}{2})}{R^2}\right)\right]\chi^{\nu}_{\kappa}(R)$$
$$+\left[1+\tfrac{1}{12}h^2\left(\frac{C^{\nu\nu}_{\kappa\kappa}}{R+h}-\frac{(\kappa+\frac{3}{2})(\kappa+\frac{5}{2})}{(R+h)^2}\right)\right]\chi^{\nu}_{\kappa}(R+h)$$
$$+h^2\left(\tfrac{1}{12}\sum_{\kappa',\,\nu'\neq\kappa,\,\nu}\frac{C^{\nu\nu'}_{\kappa\kappa'}\chi^{\nu'}_{\kappa'}(R-h)}{R-h}+\tfrac{5}{6}\sum_{\kappa',\,\nu'\neq\kappa,\,\nu}\frac{C^{\nu\nu'}_{\kappa\kappa'}\chi^{\nu'}_{\kappa'}(R)}{R}+\tfrac{1}{12}\sum_{\kappa',\,\nu'\neq\kappa,\,\nu}\frac{C^{\nu\nu'}_{\kappa\kappa'}\chi^{\nu'}_{\kappa'}(R+h)}{R+h}\right)$$
$$=-\epsilon h^2\left[\tfrac{1}{12}\chi^{\nu}_{\kappa}(R-h)+\tfrac{5}{6}\chi^{\nu}_{\kappa}(R)+\tfrac{1}{12}\chi^{\nu}_{\kappa}(R+h)\right]\cdots. \tag{2}$$

The boundary conditions are

$$\chi^{\nu}_{\kappa}(R)\sim\alpha_{\kappa\nu}R^{\kappa+3/2+1}\quad\text{as } R\to 0$$
$$\sim e^{-|\epsilon|^{1/2}R}\quad\text{as } R\to\infty\,. \tag{3}$$

$R=nh$ is the pivot point, and $\epsilon=2E$; h is the mesh size, and n is an integer.

The procedure used to solve Eqs. (2) is to determine the value of the coupled functions at the pivot point $n+1$ from a knowledge of the values of these functions at the pivots n and $n-1$. The dimension of the matrix to be solved at each pivot is equal to the number of coupled equations. This method allows the increase of the number of pivots more easily than the method of Winter *et al.*,[6] where the matrix corresponding to the total number of pivots is diagonalized (the dimension of the matrix, which is the number of pivots times the number of coupled equations, can give rise to difficult storage problems in the computer memory). We distinguish four regions in the radial solutions (see Fig. 1):

(i) The first region, with $R_1\sim 0.5$, necessitates a fine mesh size ($h\sim 0.05$).

(ii) The second and third region necessitate an intermediate mesh size ($h\sim 0.1$).

(iii) The fourth region, where the coupled curves are very smooth, only requires a relatively large mesh size ($h\sim 0.4$).

As explained by Fox,[8] we consider the forward and the backward curves, and instead of matching the solutions and their derivatives at a point R_c, we have chosen to match the solutions at two points R_{c1} and $R_{c2}=R_{c1}+mh$ (m is an integer and h the mesh size of the intermediate region). There is an evident difficulty[8] in the choice of the matching point R_c, and we believe that the best way is to choose R_c in the region where the derivatives of the coupled functions with respect to ϵ are of the same order of magnitude $|(\partial/\partial\epsilon)_f\chi^{\nu}_{\kappa}|\approx|(\partial/\partial\epsilon)_b\chi^{\nu}_{\kappa}|$ [see Eqs. (6); the left-hand subscript f refers to the forward solutions, and the left-hand subscript b refers to the backward solutions]. Figure (2) shows the drawback of matching too far to the right. Instead of getting curves like a and b which match together, one can get curves like c and b or d and b. Similar considerations apply when the matching point is too far to the left, where the backward solutions can behave like $1/R^{\kappa+3/2}$ instead of $R^{\kappa+3/2+1}$ as $R\to 0$.

We start the step-by-step iterations by assuming arbitrary but reasonable values to the different functions ${}_f\chi^{\nu}_{\kappa}(R)$,

$${}_f\chi^{\nu}_{\kappa}(0)=0,\quad {}_f\chi^{\nu}_{\kappa}(h)=f^{\nu}_{\kappa}\,, \tag{4}$$

where the f^{ν}_{κ} are the numerical values of the ${}_f\chi^{\nu}_{\kappa}$ functions at the first pivot point. By repeated use of Eqs. (2), the values of the coupled functions ${}_f\chi^{\nu}_{\kappa}(R_{c1})$ and ${}_f\chi^{\nu}_{\kappa}(R_{c2})$ are calculated. These values depend on the starting parameters ($\epsilon, f^0_0, f^1_2, f^2_4, f^0_4, \ldots$). Similarly, we start the backward solu-

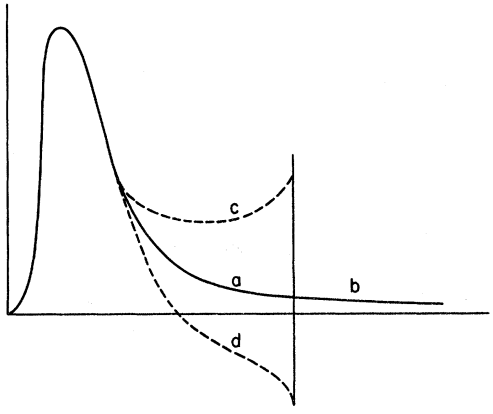

FIG. 2. Mismatch resulting when the matching point is too far to the right along the radial curve. Curves a and b show the normal behavior of a radial solution.

tions with boundary conditions

$$ {}_b\chi_\kappa^\nu(R_4) = b_\kappa^\nu, \quad {}_b\chi_\kappa^\nu(R_4 - h) = e^{|\epsilon|^{1/2}h} b_\kappa^\nu , \tag{5} $$

where R_4 stands for the end point of the range of iteration. Repeated use of Eqs. (2) in the backward direction allows the calculation of ${}_b\chi_\kappa^\nu(R_{c1})$, ${}_b\chi_\kappa^\nu(R_{c2})$, which in general will depend on the parameters $(\epsilon, b_0^0, b_2^1, b_4^2, \ldots)$. The correction $\delta\epsilon$ to the eigenvalue is calculated from Newton's formula

$$ {}_f\chi_\kappa^\nu(R_{c1}) - {}_b\chi_\kappa^\nu(R_{c1}) + \delta\epsilon\left(\frac{\partial}{\partial\epsilon}\,{}_f\chi_\kappa^\nu\Big|_{R=R_{c1}} - \frac{\partial}{\partial\epsilon}\,{}_b\chi_\kappa^\nu\Big|_{R=R_{c1}}\right) + \sum_{\kappa',\,\nu'\neq 0,\,0} \delta f_{\kappa'}^{\nu'} \frac{\partial}{\partial f_{\kappa'}^{\nu'}}\,{}_f\chi_\kappa^\nu(R)\Big|_{R=R_{c1}} - \sum_{\kappa',\,\nu'} \delta b_{\kappa'}^{\nu'} \frac{\partial}{\partial b_{\kappa'}^{\nu'}}\,{}_b\chi_\kappa^\nu\Big|_{R=R_{c1}} = 0 , \tag{6} $$

with a similar set of equations at R_{c2}. We have one parameter in excess for the solution of Newton's formula, and we have chosen arbitrarily $f_0^0 = \text{const} = 1$.

The differential equations obeyed by the different partial derivatives with respect to f_κ^ν and b_κ^ν are the same as Eqs. (1), except for the derivatives with respect to ϵ, where a term $-\chi_\kappa^\nu(R)$ has to be added at the right-hand side of Eqs. (1). The boundary conditions on these derivatives are

$$ \begin{aligned}
&\frac{\partial}{\partial f_{\kappa'}^{\nu'}}\,{}_f\chi_\kappa^\nu(R)\Big|_{R=0} = 0, \\
&\frac{\partial}{\partial f_{\kappa'}^{\nu'}}\,{}_f\chi_\kappa^\nu(R)\Big|_{R=h} = \delta_{\kappa\kappa'}\delta_{\nu\nu'}, \\
&\frac{\partial}{\partial b_{\kappa'}^{\nu'}}\,{}_b\chi_\kappa^\nu(R)\Big|_{R=R_4} = \delta_{\kappa\kappa'}\delta_{\nu\nu'}, \\
&\frac{\partial}{\partial b_{\kappa'}^{\nu'}}\,{}_b\chi_\kappa^\nu(R)\Big|_{R=R_4-h} = \delta_{\kappa\kappa'}\delta_{\nu\nu'}\, e^{|\epsilon|^{1/2}h} , \\
&\frac{\partial}{\partial\epsilon}\,{}_f\chi_\kappa^\nu(R)\Big|_{R=0} = 0, \qquad \frac{\partial}{\partial\epsilon}\,{}_f\chi_\kappa^\nu(R)\Big|_{R=h} = 0 , \\
&\frac{\partial}{\partial\epsilon}\,{}_b\chi_\kappa^\nu(R)\Big|_{R=R_4} = 0, \\
&\frac{\partial}{\partial\epsilon}\,{}_b\chi_\kappa^\nu(R)\Big|_{R=R_4-h} = -\frac{b_\kappa^\nu h}{2|\epsilon|^{1/2}}\, e^{h|\epsilon|^{1/2}} .
\end{aligned} \tag{7} $$

Equations (6), together with a similar set of equations at R_{c2}, give a system of simultaneous linear algebraic equations which are solved by using the Gauss-Jordan elimination procedure for the unknowns $\delta\epsilon, \delta f_{\kappa'}^{\nu'}, \delta b_{\kappa'}^{\nu'}$. New values $\epsilon + \delta\epsilon$, $f_{\kappa'}^{\nu'} + \delta f_{\kappa'}^{\nu'}$, $b_{\kappa'}^{\nu'} + \delta b_{\kappa'}^{\nu'}$ are calculated and the process repeated until, say $|\delta\epsilon| < 10^{-10}$.

RESULTS AND DISCUSSIONS

Figures 3–5 show the shape of the radial curves for $\kappa_{\max} = 4, 8, 12$, respectively. The correspondence between the numbering of the curves and the value

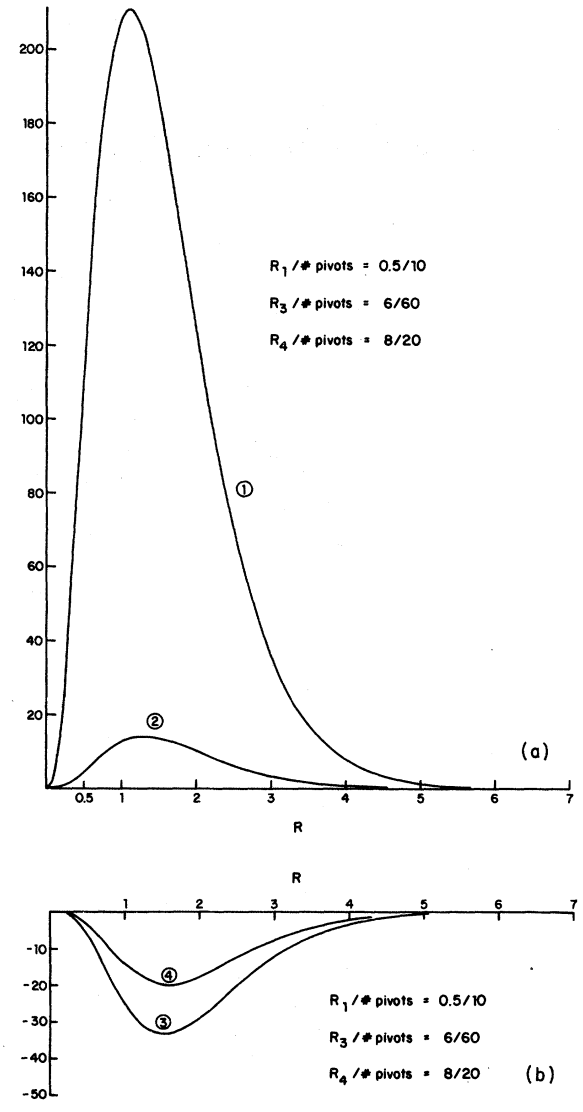

FIG. 3. Partial waves for $\kappa_{\max} = 4$. An explanation of the numbering of the curves is given in Table I. (a) Curves 1 and 2; (b) curves 3 and 4.

(κ, ν) is given in Table I. These curves show clearly that the zero-order wave function has a dominant contribution in the approximation of the wave function compared with the contribution of the higher-order partial waves. (We have the following relations between the maxima of the curves; $\chi_2^1 = 0.065\chi_0^0$, $\chi_4^2 = 0.176\chi_0^0$, $\chi_4^0 = 0.108\chi_0^0$, $\chi_6^3 = 0.001\chi_0^0$, $\chi_8^4 = 0.037\chi_0^0$.) However, an examination of Table II shows that a very large number of these curves are needed to make the ground-state energy of He converge (compare the trend of convergence of the results shown in the last column of Table II with the value of -2.9033 a.u. reported by Pekeris[9]). Erens *et al.*,[4] in their study of the triton problem, conclude similarly that although the first few partial waves might seem to give a good approximation of the wave function, indeed a very large number of these partial waves

TABLE I. Relation between the values of (κ, ν) and the numbering of the curves.

	(κ,ν)		(κ,ν)		(κ,ν)		(κ,ν)		(κ,ν)
1	(0,0)	6	(6,1)	11	(10,3)	16	(12,0)	21	(16,8)
2	(2,1)	7	(8,4)	12	(10,1)	17	(14,7)	22	(16,6)
3	(4,2)	8	(8,2)	13	(12,6)	18	(14,5)	23	(16,4)
4	(4,0)	9	(8,0)	14	(12,4)	19	(14,3)	24	(16,2)
5	(6,3)	10	(10,5)	15	(12,2)	20	(14,1)	25	(16,0)

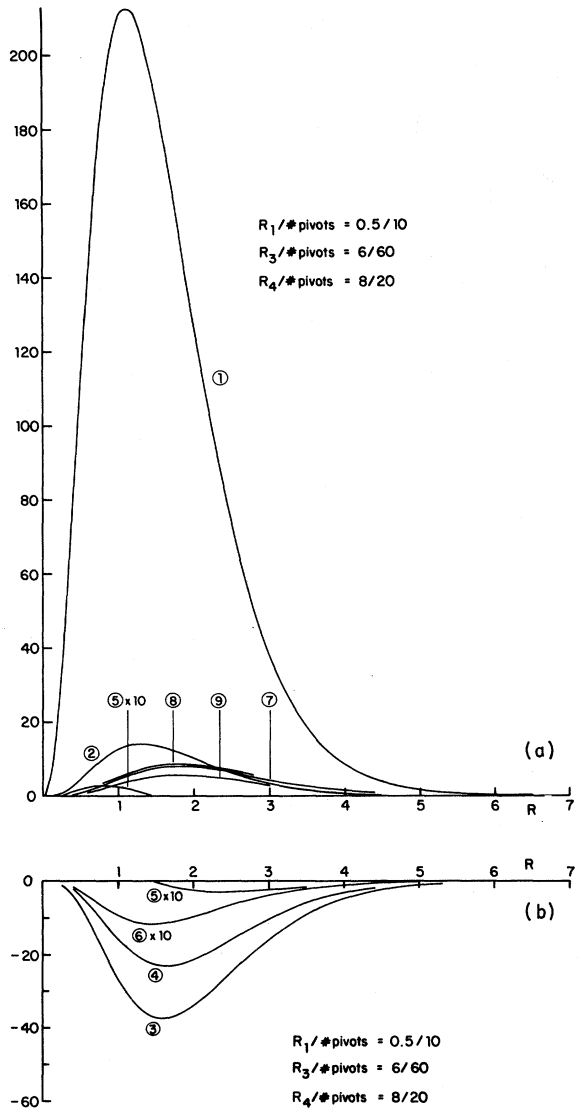

FIG. 4. Partial waves for $\kappa_{max} = 8$. (a) Curves 1, 2, 5, and 7–9; (b) curves 3–5 and 6.

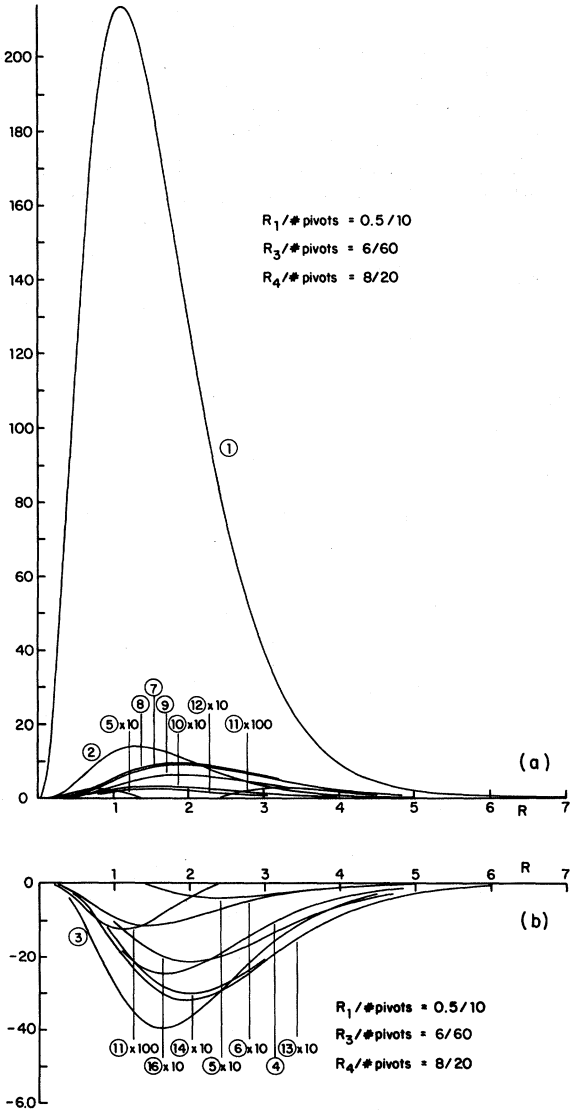

FIG. 5. Partial waves for $\kappa_{max} = 12$. (a) Curves 1, 2, 5, and 7–12; (b) curves 3–6, 11, 13, 14, and 16.

TABLE II. Variation of the characteristic value $\epsilon/2$ with κ_{max}. N_P is the number of pivots; h is the mesh size.

	κ_{max}	R_1/N_P	R_3/N_P	R_4/N_P	$R_{c1}=N_P h$	$R_{c2}=N_P h$	$\epsilon/2$ (a.u.)
1	4	0.5/10	6/60	8/20	9×0.1	10×0.1	−2.783 975 5
2	6	0.5/10	6/60	8/20	9×0.1	10×0.1	−2.784 607 6
3	8	0.5/10	10/200	24/60	25×0.05	26×0.05	−2.849 821 6
4	8	0.5/10	2/40	10/200	25×0.05	26×0.05	−2.849 821 6
5	8	0.5/10	6/60	10/25	10×0.1	15×0.1	−2.849 812 9
6	8	0.5/10	6/60	8/20	9×0.1	10×0.1	−2.849 812 9
7	8	0.5/10	6/60	8/20	20×0.1	25×0.1	−2.849 812 9
8	8	0.8/20	6.4/80	8/25	24×0.08	26×0.08	−2.849 805 4
9	8	0.8/20	6.4/80	8/25	11×0.08	12×0.08	−2.849 805 4
10	8	0.8/20	6.4/80	8/25	10×0.08	12×0.08	−2.849 805 4
11	8	0.7/20	5.6/80	8.4/30	13×0.07	14×0.07	−2.849 804 4
12	10	0.5/10	6/60	8/20	9×0.1	10×0.1	−2.849 975 1
13	12	0.5/10	6/60	8/20	8×0.1	10×0.1	−2.875 603 3
14	12	0.8/20	6.4/80	8/25	11×0.08	12×0.08	−2.875 595 5
15	16	0.5/10	6/60	8/20	8×0.1	9×0.1	−2.887 137 6
16	16	0.8/20	6.4/80	8/25	11×0.08	12×0.08	−2.887 130 5
17	20	0.5/10	6/60	8/20	8×0.1	10×0.1	−2.892 xxx x

is needed to get a good convergence of the energy value.

The results of Table II are summarized as follows:

(i) The effect on the eigenvalue of varying the mesh size of region 1 (see Fig. 1) from 0.05 to 0.04 and 0.035 is shown for the case $\kappa_{max}=8$ (lines 6, 9, and 11 of Table II). The effect on the eigenvalue of the variation of the mesh size of region 1 from 0.05 to 0.04 is also shown for the cases $\kappa_{max}=12$ and $\kappa_{max}=16$. The improvement in the accuracy of the eigenvalue in all three cases is of the order of 10^{-5} or less.

(ii) Lines 3 and 4 (compared, for instance, to line 5) show the effect of round-off errors on the eigenvalue when the number of pivots becomes large. The error is of the order of 10^{-5}. One loses about 3 digits accuracy in the numerical values of the radial functions for every 50 pivots.

(iii) Comparison of the results for $\kappa_{max}=10$ with those for $\kappa_{max}=8$ and $\kappa_{max}=12$, and $\kappa_{max}=6$ with those of $\kappa_{max}=4$ and $\kappa_{max}=8$ suggests the idea that some terms contribute poorly to the improvement of the eigenvalue. The inclusion of the partial waves $(\kappa,\nu)=(10,5)$, $(10,3)$, $(10,1)$ or $(\kappa,\nu)=(6,3)$, $(6,1)$ gives little improvement in the eigenvalue ($\kappa_{max}/2$ is odd).

To explain this, we notice that for a heavy nucleus system as in the case of He, $\delta\approx\pi/4$ (see Appendix B, Paper I), and when $r_{13}\to 0$ or $r_{23}\to 0$ (collision of an electron with the nucleus), $\lambda=\pm\pi/2$ [see Eqs. (B1), Paper I]. Our orthonormal set of functions developed in Paper I involves the function $\cos\nu\lambda$, and $\cos(\nu\pi/2)=0$ for ν odd, which corresponds to the case $\kappa_{max}/2$ odd. Thus we see that the partial waves for odd values of ν are minima at points of singularity of the potential, where the partial waves are expected on physical grounds to have large amplitude because of the attractive nature of the potential. The behavior of the eigenvalue as noted above testifies to the correctness of the numerical solution, since the functions of the internal angles ψ,λ have been eliminated, and the mentioned physical effect is indirectly reflected in the radial equations through the influence of the coupling coefficients. In the case of the triton, the three masses are equal and $\delta=\pi/3$; the results of Erens *et al.*[4] show that in this case the main

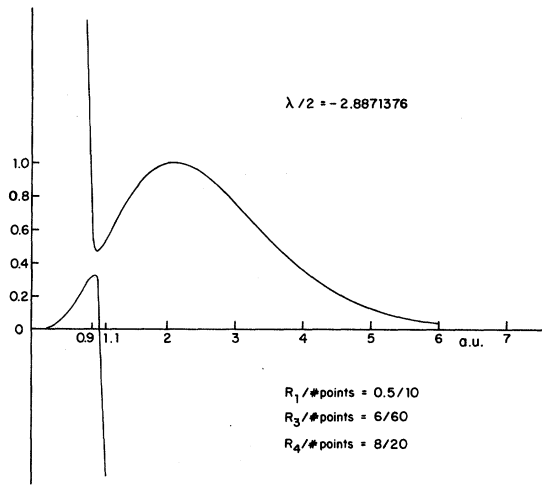

FIG. 6. A typical example of a mismatch occurring for the high-order curves for $\kappa_{max}=16$, $\nu=0$. The scale in this figure is 50 times larger than the scale in Fig. 5.

TABLE III. Relation between the correction $\delta\epsilon$, calculated from Newton's formula, and the matching of the partial waves for $\kappa_{max}=8$ (this is the result shown on line 11, Table II). Note the improvement in the matching as $\delta\epsilon$ gets smaller.

$R_{1/N_P}=0.7/20$, $R_{3/N_P}=5.6/80$, $R_{4/N_P}=8.4/30$								
	$\epsilon/2=-2.849\,7927$, $\lvert\delta\epsilon\rvert\sim 10^{-5}$		$\epsilon/2=-2.849\,800\,07$, $\lvert\delta\epsilon\rvert\sim 10^{-6}$			$\epsilon/2=2.849\,804\,4$, $\lvert\delta\epsilon\rvert<10^{-7}$		
(κ,ν)	${}_b\chi^{\nu}_{\kappa}-{}_f\chi^{\nu}_{\kappa}(14\times 0.07)$	(κ,ν)	${}_b\chi^{\nu}_{\kappa}-{}_f\chi^{\nu}_{\kappa}(13\times 0.07)$	${}_b\chi^{\nu}_{\kappa}-{}_f\chi^{\nu}_{\kappa}(14\times 0.07)$	(κ,ν)	${}_b\chi^{\nu}_{\kappa}-{}_f\chi^{\nu}_{\kappa}(13\times 0.07)$	${}_b\chi^{\nu}_{\kappa}-{}_f\chi^{\nu}_{\kappa}(14\times 0.07)$
$\left(13\times\frac{5.6}{80}\right)$							
(0, 0)	-0.3442×10^{-2}	(0, 0)	-0.1288×10^{-2}	-0.1453×10^{-3}	(0, 0)	0.1048×10^{-4}	0.1179×10^{-5}
(2, 1)	0.6053×10^{-2}	(2, 1)	0.2266×10^{-2}	-0.6082×10^{-4}	(2, 1)	-0.1843×10^{-4}	0.5093×10^{-6}
(4, 2)	-0.9091×10^{-2}	(4, 2)	-0.3403×10^{-2}	0.1177×10^{-2}	(4, 2)	0.2767×10^{-4}	-0.9605×10^{-5}
(4, 0)	0.1879×10^{-1}	(4, 0)	0.7035×10^{-2}	$0.693\,03\times10^{-3}$	(4, 0)	-0.5724×10^{-4}	$-0.564\,08\times10^{-5}$
(6, 3)	0.2523×10^{-1}	(6, 3)	0.9447×10^{-2}	-0.3926×10^{-3}	(6, 3)	-0.7685×10^{-4}	0.3223×10^{-5}
(6, 1)	-0.2014×10^{-1}	(6, 1)	-0.7551×10^{-2}	0.4011×10^{-4}	(6, 1)	$0.614\,03\times10^{-4}$	-0.3954×10^{-6}
(8, 4)	-0.3684	(8, 4)	-0.1379	0.6632×10^{-2}	(8, 4)	0.1122×10^{-2}	-0.5346×10^{-4}
(8, 2)	0.3997	(8, 2)	0.1496	0.5084×10^{-2}	(8, 2)	-0.1216×10^{-2}	-0.4002×10^{-4}
(8, 0)	0.6911×10^{-1}	(8, 0)	0.2587×10^{-1}	0.36×10^{-2}	(8, 0)	-0.212×10^{-3}	-0.3225×10^{-4}

contribution to the convergence of the energy comes from partial waves for which ν is a multiple of 3.

(iv) The matching of the forward and backward curves has been carried out successfully for all cases up to and including $\kappa_{max}=12$ (16 coupled curves). A slight mismatch occurs for the high-order curves for the case $\kappa_{max}=16$ (25 coupled curves) that we have been unable to overcome. Probably a finer mesh size should be chosen for regions 2 and 3 (Fig. 1), but this point requires a little more study. A typical example of the mismatch which occurs for these high-order curves is shown in Fig. 6.

Usually by repeated application of Newton's formula [Eqs. (6)] the matching of the low-order curves takes place first, and the matching of the high-order curves follows. A look at Table III gives an idea of the relation between the magnitude of the correction $\delta\epsilon$ as calculated by Newton's formula [Eqs. (6)] and the slight mismatch occurring in the high-order curves (8,4) and (8,2). The magnitude of $\delta\epsilon$ gets smaller as the matching improves. It must be noted that the rate of change of the derivatives (which determines the shape of the coupled curves) is controlled by the second-order derivatives, which, from Eqs. (1), can be expressed as a sum of a diagonal term and a nondiagonal term,

$$-\sum_{(\kappa',\nu')\neq(\kappa,\nu)} C^{\nu\nu'}_{\kappa\kappa'}\,\frac{\chi^{\nu'}_{\kappa'}(R)}{R}\ ,$$

and a slight inaccuracy in the partial waves affects the second-order derivatives, without affecting appreciably the eigenvalue (the effect on the eigenvalue is of the second order or less for an error of the first order in the partial waves).

(v) A superposition of the curves of Figs. 3–5 shows visually little effect on the low-order curves (small ν and κ) as higher-order curves are added (κ_{max} increasing). That is to say, our calculations indicate a lack of sensitivity of the radial functions to truncation of the series expansion. Although we have no analytic justification why this is so, we believe that our low-order functions represent well those that would result from the actual (nontruncated) solution of the He problem.

CONCLUSION

The numerical integration for the forward and backward solutions of the set of coupled ordinary differential equations for the He atom has been successfully carried out for up to 16 coupled curves, and the method would probably work to match 18 or 20 radial curves. The radial solutions shown in Figs. 3–5 are not sensitive to the truncation of the series and consequently are likely

truly representative of the coefficients of the expansion of the wave function. However, to obtain the required accuracy in the eigenvalue is beyond the possibility of computations. High values of κ_{max} not only make the problem of the matching of the curves difficult, but also introduce problems of round-off errors, because of the large matrices involved in the calculation. Besides, the total CPU time on an IBM/370/158 machine for one iteration (70 pivots) is of the order of 25.25 sec for $\kappa_{max}=6$, 32 sec for $\kappa_{max}=8$, 40.5 sec for $\kappa_{max}=10$, 85.5 sec for $\kappa_{max}=12$, 185 sec for $\kappa_{max}=16$, 394 sec for $\kappa_{max}=20$; the increase in CPU time becomes very rapid for large κ_{max}. It may be noted that the approach developed here compares favorably with the method of Winter *et al.*[6] For all $\kappa_{max}\leq 12$, only around 70 pivots are necessary to get an adequate convergence of the eigenvalue (a four-decimal accuracy). This is to be compared with the 60×60 pivots used by Winter *et al.*,[6] which gave a value of $-2.808\,902$ a.u. and required diagonalization of a 3600×3600 matrix. In contrast, in the method used here the number of iterations (application of Newton's corrections) required to get $|\delta\epsilon|$ smaller, say, than 10^{-10} becomes excessive for large κ_{max}. But this number is reasonable for κ_{max} less than or equal to 12 (around 10 iterations or less). It is important that proper starting values be assumed, and we believe that the best way to do this is to proceed gradually from $\kappa_{max}=4$ to $\kappa_{max}=6, 8, 10$ and higher values.

ACKNOWLEDGMENTS

We gratefully acknowledge helpful discussions concerning the numerical aspect of this work with G. Tenti and J. Mehaffey, Department of Physics, University of Toronto, I. Farkas, Department of Computer Sciences, University of Toronto, R. Miville-Deschenes, Centre de Traitement de l'Information, Université Laval, J. Bergeron, Département d'Informatique, Université Laval, and M. Fortin, Département des Mathématiques, Université Laval. The interest of M. de Celles, Département de Physique, Université Laval, is also gratefully acknowledged. This work was partly started when one of us (R.M.S.) was at the Department of Physics, University of Toronto, and we we would like to thank Professor J. Van Kranendonk for the continuous assistance, interest, and encouragement he showed during this period.

APPENDIX A

In this appendix, we give the expression used to calculate the matrix elements $C^{\nu\nu'}_{\kappa\kappa'}$. The potential function is given by

$$V=\frac{e^2}{r_{12}}-\frac{Ze^2}{r_{13}}-\frac{Ze^2}{r_{23}}\quad . \tag{A1}$$

The expression of the interparticle distances in terms of R has been derived by De Celles and Darling.[10] Making use of these relations, one can easily get

$$\frac{C^{\nu\nu'}_{\kappa\kappa'}}{R}=-2\int_0^1\int_0^{2\pi} u^{\nu}_{\kappa}(\lambda,\psi)\left(\frac{e^2}{r_{13}}-\frac{Ze^2}{r_{13}}-\frac{Ze^2}{r_{23}}\right)u^{\nu'}_{\kappa'}(\lambda,\psi)\pi^2\rho\,d\rho\,d\lambda\ , \tag{A2}$$

$$C^{\nu\nu'}_{\kappa\kappa'}=2Ze^2\,(2\mu)^{1/2}\int_0^1\int_0^{2\pi} u^{\nu}_{\kappa}\left(\frac{1}{[1+\cos\psi\cos(\lambda-2\delta)]^{1/2}}+\frac{1}{[1+\cos\psi\cos(\lambda+2\delta)]^{1/2}}\right)u^{\nu'}_{\kappa'}\,\pi^2\rho\,d\rho\,d\lambda$$

$$-2e^2(m_e)^{1/2}\int_0^1\int_0^{2\pi} u^{\nu}_{\kappa}\frac{1}{(1+\cos\psi\cos\lambda)^{1/2}}\,u^{\nu'}_{\kappa'}\,\pi^2\rho\,d\rho\,d\lambda\ . \tag{A3}$$

The right-hand side of expression (A3) has to be divided by $e^2(m_e)^{1/2}/\hbar^2$ if it is to be expressed in atomic units [note that in Eq. (A3), $\hbar=1$]. Taking into account the expression of $u^{\nu}_{\kappa}(\lambda,\psi)$ [Eqs. (24), I], one can write Eq. (A3) as

$$C^{\nu\nu'}_{\kappa\kappa'}=2Ze^2(2\mu)^{1/2}[(\kappa+2)(\kappa'+2)]^{1/2}\frac{\delta_{\nu}\delta_{\nu'}}{\pi}$$

$$\times\int_0^1\rho^{\nu'}P^{\nu',0}_{(\kappa/2-\nu')/2}(1-2\rho^2)P^{\nu,0}_{(\kappa/2-\nu)/2}(1-2\rho^2)\rho\,d\rho\int_0^{2\pi}\left(\frac{\cos\nu\lambda\cos\nu'\lambda}{[1+\rho\cos(\lambda+2\delta)]^{1/2}}+\frac{\cos\nu\lambda\cos\nu'\lambda}{[1+\rho\cos(\lambda-2\delta)]^{1/2}}\right)d\lambda$$

$$-2e^2(m_e)^{1/2}[(\kappa+2)(\kappa'+2)]^{1/2}\frac{\delta_{\nu}\delta_{\nu'}}{\pi}$$

$$\times\int_0^1\rho^{\nu'}P^{\nu',0}_{(\kappa/2-\nu')/2}(1-2\rho^2)\rho^{\nu}P^{\nu,0}_{(\kappa/2-\nu)/2}(1-2\rho^2)\rho\,d\rho\int_0^{2\pi}\frac{\cos\nu\lambda\cos\nu'\lambda}{(1+\rho\cos\lambda)^{1/2}}\,d\lambda\ . \tag{A4}$$

The expression of the Jacobi polynomials $P^{\nu,0}_{\frac{1}{2}(\kappa/2-\nu)}$ is given by[11]

$$P^{\nu,0}_{(\kappa/2-\nu)/2}(1-2\rho^2)=\sum_{r=0}^{(\kappa/2-\nu)/2}\frac{\Gamma(1+(\kappa/2+\nu)/2+r)(-1)^r\rho^{2r}}{r![(\kappa/2-\nu)/2-r]!\Gamma(1+\nu+r)}\ . \tag{A5}$$

Making use of the relation $\cos\nu\lambda\cos\nu'\lambda=\frac{1}{2}[\cos(\nu+\nu')\lambda+\cos|\nu-\nu'|\lambda]$,

$$C^{\nu\nu'}_{\kappa\kappa'}=4Ze^2(2\mu)^{1/2}[(\kappa+2)(\kappa'+2)]^{1/2}\frac{\delta_\nu\delta_{\nu'}}{\pi}\tfrac{1}{2}[J^{\nu\nu'}_{\kappa\kappa'}(l)\cos2l\delta+J^{\nu\nu'}_{\kappa\kappa'}(l')\cos2l'\delta]$$
$$-2e^2(m_e)^{1/2}[(\kappa+2)(\kappa'+2)]^{1/2}\frac{\delta_\nu\delta_{\nu'}}{\pi}\tfrac{1}{2}[J^{\nu\nu'}_{\kappa\kappa'}(l)+J^{\nu\nu'}_{\kappa\kappa'}(l')]\ , \tag{A6}$$

where $l=\nu+\nu'$, $l'=|\nu-\nu'|$, and

$$J^{\nu\nu'}_{\kappa\kappa'}(l)=\int_0^1\int_0^{2\pi}\frac{\cos l\lambda}{(1+\rho\cos\lambda)^{1/2}}\rho^{\nu'}P^{\nu',0}_{(\kappa'/2-\nu')/2}(1-2\rho^2)\rho^{\nu}P^{\nu,0}_{(\kappa/2-\nu)/2}(1-2\rho^2)\,\pi^2\rho\,d\rho\,d\lambda\ . \tag{A7}$$

By expanding the quantity $(1+\rho\cos\lambda)^{-1/2}$, it is easy to show that[12]

$$\int_0^{2\pi}\frac{\cos l\lambda}{(1+\rho\cos\lambda)^{1/2}}\,d\lambda=2(-1)^l\frac{\pi\rho^l}{2^{3l}}\frac{(2l)!}{l!l!}F(\tfrac{1}{4}(2l+1),\tfrac{1}{4}(2l+3);1+l;\rho^2)\ , \tag{A8}$$

where $F(\frac{1}{4}(2l+1),\frac{1}{4}(2l+3);1+l;\rho^2)$ is the Gauss hypergeometric function. Equation (A7) can be written as

$$J^{\nu\nu'}_{\kappa\kappa'}=(-1)^l\frac{\pi^2}{2}\sum_{r=0}^{(\kappa/2-\nu)/2}\frac{\Gamma(1+(\kappa/2+\nu)/2+r)(-1)^r}{r![(\kappa/2-\nu)/2-r]!\Gamma(1+\nu+r)}$$
$$\times\sum_{r'=0}^{(\kappa'/2-\nu')/2}\frac{\Gamma(1+(\kappa'/2+\nu')/2+r')(-1)^{r'}}{r'![(\kappa'/2-\nu')/2-r']!\Gamma(1+\nu'+r')}I_l(r+r'), \tag{A9}$$

where

$$I_l(r+r')=\frac{2\pi}{2^{3l}}\frac{(2l)!}{l!l!}\int_0^1 z^l F(z)z^{r+r'}\,dz\ . \tag{A10}$$

$z=\rho^2\cdot I_l(r+r')$ is calculated using the recurrence relations

$$I_l(r+r')=\frac{16\sqrt{2}}{(2l+1)(2l+3)+16(r+r')(l+r+r'+1)}+\frac{16(r+r')(l+r+r')}{(2l+1)(2l+3)+16(r+r')(l+r+r'+1)}I_l(r+r'-1)\ , \tag{A11}$$

$$I_l(0)=16\sqrt{2}/(2l+1)(2l+3)\ . \tag{A12}$$

APPENDIX B

We give here briefly the connection between the independent variables used in this work and the work of Simonov,[2] since these two works develop the two main methods used to derive the coupled set of equations (1). The starting equations in the work of Simonov are

$$\vec{\eta}=(\vec{r}_1-\vec{r}_2)/\sqrt{2}\ , \tag{B1}$$
$$\vec{\xi}=\sqrt{\tfrac{2}{3}}\,[\tfrac{1}{2}(\vec{r}_1+\vec{r}_2)-\vec{r}_3]\ . \tag{B2}$$

Using the variables R, ψ, and $\chi=\lambda/2$, one can easily show that[10]

$$\eta_x=m_e^{1/2}R\cos(\psi/2)\cos\chi\ ,$$
$$\eta_y=-m_e^{1/2}R\sin(\psi/2)\sin\chi\ , \tag{B3}$$
$$\eta^2=\tfrac{1}{2}m_eR^2(1+\cos\psi\cos2\chi)\ ,$$
$$\xi_x=m_e^{1/2}R\cos(\psi/2)\sin\chi\ ,$$
$$\xi_y=m_e^{1/2}R\sin(\psi/2)\cos\chi\ , \tag{B4}$$
$$\xi^2=\tfrac{1}{2}m_eR^2(1-\cos\psi\cos2\chi)\ .$$

The angle φ in the work of Simonov[2] is given by

$$\cos\varphi=\frac{\xi_x\eta_x+\xi_y\eta_y}{\xi\eta}=\frac{\sin2\chi\cos\psi}{(1-\cos^2\psi\cos^22\chi)^{1/2}}\ . \tag{B5}$$

The quantity mR^2 is equivalent to ρ^2 in the work of Simonov,[2] and the angle θ of Simonov[2] is given by

$$\cos\theta=\tfrac{1}{2}\sqrt{2}\,(1+\cos\psi\cos2\chi)^{1/2}\ ,$$
$$\sin\theta=\tfrac{1}{2}\sqrt{2}\,(1-\cos\psi\cos2\chi)^{1/2}\ . \tag{B6}$$

The variable A and λ in the work of Simonov[2] are given by

$$A^2 = \cos^2 2\theta + \sin^2 2\theta \cos^2\varphi = \cos^2\psi \ ,$$

$$\cos\lambda = (\cos 2\theta)/A = \cos 2\chi \ , \tag{B7}$$

$$\sin\lambda = (\sin 2\theta \cos\varphi)/A = \sin 2\chi \ ,$$

$$\lambda = 2\chi \ ;$$

$$-\pi \leq \lambda \leq \pi$$

and[13]

$$-\pi/2 \leq \chi \leq \pi/2 \ .$$

APPENDIX C

The boundary conditions given in Eqs. (7) are valid for the reduced function $\Psi_r = \sum_{\kappa,\nu} \chi_\kappa^\nu(R) u_\kappa^\nu(\lambda,\psi)$, i.e., the function Ψ_r is a solution of the reduced KEO [for the definition of the reduced KEO, see footnote (5) of part I and reference (10)]. By direct application of the definition given in reference (10), p. 73, it can be shown that the non-reduced function Ψ is related to the reduced function Ψ_r by relation $\Psi = \Psi_r / R^{5/2}$. The important result is that when $R \to 0$, $\chi_0^0/R^{5/2} \to \alpha_{00} \neq 0$, as it should be, while $\chi_\kappa^\nu/R^{5/2} \to 0$ for $(\kappa,\nu) \neq (0,0)$.

---

*Work based on a thesis submitted by R. M. Shoucri in partial fulfillment of the requirements for the degree of Doctor of Philosophy in Physics, Université Laval, Québec. This work has been supported by a grant from the National Research Council of Canada.

[1]B. T. Darling and R. M. Shoucri, preceding paper, Phys. Rev. A 12, 2264 (1975).
[2]Yu. A. Simonov, Yadern. Fiz. 3, 630 (1966) [Sov. J. Nucl. Phys. 3, 461 (1966)].
[3]D. D. Brayshaw and B. Buck, Phys. Rev. Lett. 24, 733 (1970).
[4]G. Erens, J. L. Visschers, and R. Van Wageningen, Ann. Phys. (N.Y.) 67, 461 (1971).
[5]J. Bruinsma and R. Van Wageningen, Phys. Lett. 44B, 221 (1973).
[6]N. W. Winter, A. Laferrière, and V. McKoy, Phys. Rev. A 2, 49 (1970).
[7]A. C. Allison, J. Comput. Phys. 6, 378 (1970).
[8]L. Fox, *Numerical Solution of Ordinary and Partial Differential Equations* (Pergamon, New York, 1962).
[9]C. L. Pekeris, Phys. Rev. 126, 1470 (1962).
[10]M. De Celles and B. T. Darling, J. Mol. Spectrosc. 29, 66 (1969).
[11]E. Rainville, *Special Functions* (MacMillan, New York, 1960).
[12]T. H. Gronwall, Phys. Rev. 51, 655 (1937).
[13]In Ref. 10, the range of the angle χ is to be accordingly corrected.